

Supporting Information

Computational Details

Computations were carried out using the Gaussian 09 program suite.¹ The structure optimizations (see Figure S1-S18) are performed with B3PW91 functional with 6-31G(d,p) basis set and characterized to be true local energy minima on the potential energy surface and no imaginary frequencies were found. Heat of formation (HOF) is a measure of energy content of an energetic material that can decompose, ignite and explode by heat or impact. It enters into the calculation of explosive and propellant properties such as detonation velocity, detonation pressure, heat of detonation and specific impulse. However, it is impractical to determine the HOF of novel energetic materials because of their unstable intermediates and unknown combustion mechanism. The calculated total energies (E_0), zero point energies (ZPE), and thermal corrections (H_T) at the B3PW91/6-31G(d,p) level for the reference compounds used in isodesmic reactions are listed in Table S1. Table S2 lists the total energies (E_0), zero point energies (ZPE), and thermal corrections (H_T) for oxadiazole derivatives. HOF_{Gas} has been predicted by designing appropriate isodesmic reactions (see Figure S19). In an isodesmic reaction, the number of each kind of formal bond is conserved according to bond separation reaction (BSR) rules. The target molecule is broken down into a set of heavy atom molecules containing same component bonds. BSR rules cannot be applied to the molecules with delocalized bonds and cage skeletons because of large calculated errors of HOFs. In view of the above, present study involves the design of isodesmic reactions in which the numbers of all kinds of bonds keep invariable to decrease the calculation errors of HOF. Aromatic rings are kept intact while constructing isodesmic reactions. The usage of the HOF_{Gas} in the calculation of detonation properties slightly overestimates the values of detonation velocity and detonation

pressure, and hence, the solid phase HOF ($\text{HOF}_{\text{Solid}}$) has been calculated which can efficiently reduce the errors. The $\text{HOF}_{\text{Solid}}$ is calculated as the difference between HOF_{Gas} and heat of sublimation (HOF_{Sub}) as,

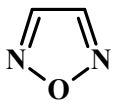
$$\text{HOF}_{\text{Solid}} = \text{HOF}_{\text{Gas}} - \text{HOF}_{\text{Sub}} \quad (1)$$

The heat of sublimation (HOF_{Sub}), which is required to convert the HOF_{Gas} to the $\text{HOF}_{\text{Solid}}$, was calculated from Equation (2),²

$$HOF_{\text{Sub}} = 0.000267 A^2 + 1.650087 (\nu \sigma_{\text{tot}}^2)^{0.5} - 2.966078 \quad (2)$$

Where A represents the surface area of the 0.001 electrons/bohr³ isosurface of electronic density, ν denotes the degree of balance between the positive and negative surface potentials, and σ_{tot}^2 is the electrostatic potential variance. These molecular surface properties were obtained using the Multiwfn program³ and listed in Table S3.

Table S1. Calculated total energies at 298K (E_0), zero point energies (ZPE), and thermal corrections (H_T) and experimental HOF_{gas} of reference compounds used isodesmic reaction at the B3PW91/6-31G(d,p) level.

Compd.	E_0 (a.u.)	ZPE (au)	H_T (au)	HOF_{gas} (kJ/mol)
	-261.899014	0.0462	0.0044	195.75 ^a

	-261.937484	0.0469	0.0044	88.76 ^a
	-466.296852	0.0488	0.0068	221.83 ^a
	-521.612111	0.0662	0.0079	257.95
CH ₄	-40.459807	0.0450	0.0039	-74.6
CH ₃ -N=N-CH ₃ (trans)	-189.119066	0.0847	0.006	152.66 ^a
CH ₃ CH ₃	-79.730092	0.075	0.0044	-84
CH ₃ NO ₂	-244.866526	0.0502	0.0053	-81
CH ₃ NHNO ₂	-300.16793	0.0679	0.0061	-3.76

^aCalculated using G4 method.

Table S2. Calculated total energies (E_0), zero point energies (ZPE), and thermal corrections (H_T) for designed compounds at the B3PW91/6-31G(d,p) level.

Compd.	E_0 (a.u.)	ZPE (a.u.)	H_T (a.u.)
O1	-670.681578	0.0511	0.0094
O2	-931.408995	0.0779	0.0129
O3	-1192.126688	0.1042	0.0167
O4	-1452.848659	0.1307	0.0204

O5	-1192.164386	0.1046	0.0167
O6	-1452.925969	0.1316	0.0204
O7	-781.318477	0.0860	0.0114
O8	-1042.045151	0.1118	0.0155
O9	-1302.764183	0.1383	0.0191
O10	-1563.480032	0.1653	0.0224
O11	-1302.801998	0.1385	0.0193
O12	-1563.566924	0.1659	0.0227
O13	-1040.783365	0.0866	0.0150
O14	-1410.884993	0.1221	0.0206
O15	-1780.985168	0.1573	0.0264
O16	-1151.421222	0.1205	0.0176
O17	-1521.521329	0.156	0.0232
O18	-1891.621990	0.1914	0.0289

Table S3. Calculated molecular surface properties of oxadiazole derivatives.

Compd.	Surface area (Å²)	Volume (Å³)	σ_{tot}^2 (kJ/mol)	ν
O1	150.16	137.66	139.01	0.0971
O2	196.85	195.86	127.17	0.1306
O3	253.42	257.20	128.08	0.1410
O4	305.75	317.15	123.89	0.1559

O5	257.49	257.07	139.76	0.1357
O6	313.13	316.76	137.71	0.1423
O7	173.55	167.24	276.45	0.1113
O8	228.12	226.72	176.78	0.1792
O9	277.45	285.38	163.42	0.1991
O10	326.73	345.73	162.65	0.2083
O11	284.08	286.38	208.07	0.1570
O12	338.95	345.67	196.26	0.1738
O13	231.83	223.78	140.64	0.1317
O14	314.26	310.37	124.94	0.1456
O15	396.48	396.83	118.60	0.1569
O16	260.75	254.75	213.10	0.1607
O17	342.96	341.19	189.37	0.1721
O18	425.32	427.75	174.16	0.1778

Surface area and volume are computed on the 0.001 au molecular surfaces. σ_{tot}^2 indicate the variability of the electrostatic potential, v is the degree of balance between the positive and the negative potentials on a molecular surface and is unitless.

The density has been referred to as “the primary physical parameter in detonation performance” of explosives.⁵⁻¹¹ For example, the important performance attribute of detonation velocity is proportional to density, while the detonation pressure is proportional to the square of the initial density.¹² An increase in density is also desirable in terms of the amount of material that can be packed into volume-limited warhead or propulsion configurations. The densities (ρ) for designed

compounds were calculated using the equation (3), as suggested by Politzer et al.¹³ for CHNO energetic compounds,

$$\rho = 0.9183 \left(\frac{M}{V_m} \right) + 0.0028 (\nu \sigma_{tot}^2) + 0.0443 \quad (3)$$

where, M is the molecular mass in g/mol. V_m is the volume enclosed by the 0.001 au contour of the molecule's electronic density and $\nu \sigma_{tot}^2$ is an electrostatic interaction index.

Oxygen balance (OB) is one of the parameter of quantifying how well an explosive provides its own oxidant.¹⁴ Most of the energy released comes from oxidation (reaction with oxygen), the amount of oxygen available is a critical factor. If excess oxygen molecules are remaining after the oxidation reaction, the oxidizer is said to have a 'positive' OB. If the oxygen molecules are completely consumed and excess fuel molecules remain, the oxidizer is said to have a 'negative' OB. If neutral OB (OB = 0%), means that there is exactly enough oxygen for the complete oxidation. It is reported that the heat of detonation (Q) reaches a maximum for an OB of zero, since this corresponds to the stoichiometric oxidation of carbon to carbon dioxide and hydrogen to water. The OB can therefore be used to optimize the composition of the explosive to give an OB as close to zero as possible. In addition, knowledge of OB in explosives can be applied in the processing of mixtures of explosives. OB (%) for an explosive containing the general formula C_aH_bN_cO_d with molecular mass M can be calculated as,

$$OB(\%) = \frac{(d - 2a - 0.5b)}{M} \times 1600 \quad (4)$$

The driving force behind the development of any new materials for the defence use is, and almost certainly will be, performance. For secondary explosives, the power of an explosive is

often described by the detonation velocity (D) and the detonation pressure (P). D reflects the velocity of the shockwave propagated by the explosive during detonation, while P is the peak dynamic pressure in the shock front. Detonation performance depends on the energy release that accompanies the decomposition and combustion processes occurring. The detonation velocity (D in km/s) and detonation pressure (P in GPa) are the performance parameters, computed using the empirical Kamlet–Jacobs equations:¹²

$$N = \frac{2c + 2d + b}{48a + 4b + 56c + 64d} \quad (5)$$

$$M = \frac{56c + 88d - 8b}{2c + 2d + b} \quad (6)$$

$$Q = \frac{28.9b + 47 \left(d - \frac{b}{2} \right) + HOF_{Explosive}}{12a + b + 14c + 16d} \quad (7)$$

$$D = 1.01(NM^{0.5}Q^{0.5})^{0.5}(1+1.30\rho) \quad (8)$$

$$P = 1.55\rho^2 NM^{0.5} Q^{0.5} \quad (9)$$

in which, N represents the moles of detonation gases per gram explosive (see Table S4), M is the average molecular weight of these gases (g/mol) (see Table S4), Q denotes the heat of detonation (cal/g), and ρ is the predicted density of salts (g/cm³).

Table S4. Calculated number of moles of detonation gases per gram of explosive (N) and average molecular weight of these gases (M) used in Kamlet-Jacobs equations for oxadiazole derivatives.

Compd.	Chemical formula	Molecular weight (g/mol)	N (mol/g)	M (g/mol)
--------	------------------	--------------------------	-----------	-----------

O1	$\text{C}_2\text{N}_4\text{O}_5$	160.04	0.028	36.889
O2	$\text{C}_4\text{N}_6\text{O}_6$	228.08	0.026	36.000
O3	$\text{C}_6\text{N}_8\text{O}_7$	296.11	0.025	35.467
O4	$\text{C}_8\text{N}_{10}\text{O}_8$	364.15	0.025	35.111
O5	$\text{C}_6\text{N}_8\text{O}_7$	296.11	0.025	35.467
O6	$\text{C}_8\text{N}_{10}\text{O}_8$	364.15	0.025	35.111
O7	$\text{C}_2\text{H}_2\text{N}_6\text{O}_5$	190.07	0.032	31.667
O8	$\text{C}_4\text{H}_2\text{N}_8\text{O}_6$	258.11	0.029	32.000
O9	$\text{C}_6\text{H}_2\text{N}_{10}\text{O}_7$	326.14	0.028	32.222
O10	$\text{C}_8\text{H}_2\text{N}_{12}\text{O}_8$	394.18	0.027	32.381
O11	$\text{C}_6\text{H}_2\text{N}_{10}\text{O}_7$	326.14	0.028	32.222
O12	$\text{C}_8\text{H}_2\text{N}_{12}\text{O}_8$	394.18	0.027	32.381
O13	$\text{C}_4\text{N}_8\text{O}_6$	256.09	0.027	34.857
O14	$\text{C}_6\text{N}_{12}\text{O}_7$	352.14	0.027	33.895
O15	$\text{C}_8\text{N}_{16}\text{O}_8$	448.19	0.027	33.333
O16	$\text{C}_4\text{H}_2\text{N}_{10}\text{O}_6$	286.12	0.030	31.529
O17	$\text{C}_6\text{H}_2\text{N}_{14}\text{O}_7$	382.17	0.029	31.455
O18	$\text{C}_8\text{H}_2\text{N}_{18}\text{O}_8$	478.22	0.028	31.407

A prime concern in the area of energetic materials (explosives and propellants) is sensitivity. Sensitivity refers to the vulnerability of a material to unintended detonation due to an accidental stimulus (impact, shock, electrical sparks, etc.).¹⁵⁻²² Sensitivity depends upon a number of different factors: molecular and crystal properties, the physical state of the compound,

environmental conditions, the nature of the stimulus, etc. Partly for these reasons, reproducibility of measured values is notoriously difficult. Experimentally, great care is required to employ very specific and uniform procedures and conditions in preparing and testing the materials; and most of the times these procedures provide crude and qualitative estimates. In view of the computational work, a large number of correlations have been established between different types of sensitivity and a remarkable array of individual molecular or crystal properties. These properties include the strengths or lengths of certain bonds, electronic energy levels, molecular electrostatic potentials, heats of fusion or sublimation, band gaps, NMR chemical shifts, the efficiencies of lattice-to-molecular vibrational energy transfer, atomic charges, electronegativities, substituent constants, etc.¹⁵⁻²² Some of these correlations are quite good, usually for nitrobenzenes and nitramines. Nevertheless they are regarded as only indicative. In the present work, we used the bond dissociation energies (BDEs), heat of detonation (Q), and balance parameter (ν) to correlate the sensitivity and stability of energetic molecules.

In energetic materials, generally, C–NO₂, N–NO₂ and O–NO₂ are the weakest bond which easily ruptures on applying external stimuli. In previous reports, evidence indicates that a key initiation step is the rupture of a specific type of bond, a “trigger linkage”. Hence, we have calculated the bond dissociation energy (BDE) of longest C–NO₂, N–NO₂ or O–NO₂ bond using following equation (10) at B3PW91/6-31G(d,p) level,

$$BDE = [E_{R1} + E_{R2}] - E_{R1-R2} \quad (10)$$

where E_{R1-R2}, E_{R1} and E_{R2} are the total energies with zero point energy correction of the precursor and the corresponding radicals produced by bond dissociation (see Table S5).

Politzer et al.^{23–25} correlated the sensitivity of energetic compounds with the imbalance (ν) between the molecular surface potentials. It is reported that the higher imbalance (ν) in the molecular surface potentials owing to the presence of more electronegative and electron-withdrawing atoms/groups present in the molecular structure indicates greater sensitivity. ν is calculated using Eq. (11) based on the strengths and variabilities of the positive (σ_+^2) and negative (σ_-^2) surface potentials and reaches a maximum of 0.250.

$$\nu = \frac{\sigma_+^2 \sigma_-^2}{(\sigma_+^2 + \sigma_-^2)^2} \quad (11)$$

Table S5. Calculated total energies (E_0) of R–NO₂, R, and NO₂ at the B3PW91/6-31G(d,p) level, used in the prediction of bond dissociation energies.

Compd.	E_0 (a.u.)		
	R–NO ₂	R	NO ₂
O1	-670.681578	-465.605075	-204.982012
O2	-931.408995	-726.327025	-204.982012
O3	-1192.126688	-987.05024	-204.982012
O4	-1452.848659	-1247.768844	-204.982012
O5	-1192.164386	-987.085913	-204.982012
O6	-1452.925969	-1247.847635	-204.982012
O7	-781.318477	-576.285319	-204.982012
O8	-1042.045151	-837.011187	-204.982012
O9	-1302.764183	-1097.730722	-204.982012

O10	-1563.480032	-1358.455101	-204.982012
O11	-1302.801998	-835.704053	-204.982012
O12	-1563.566924	-1205.804541	-204.982012
O13	-1040.783365	-1575.904508	-204.982012
O14	-1410.884993	-946.386932	-204.982012
O15	-1780.985168	-1316.486847	-204.982012
O16	-1151.421222	-1686.587477	-204.982012
O17	-1521.521329	-1097.769029	-204.982012
O18	-1891.621990	-1358.532121	-204.982012

References

1. Gaussian 09, Revision E.01, M. J. Frisch, G. W. Trucks, H. B. Schlegel, G. E. Scuseria, M. A. Robb, J. R. Cheeseman, G. Scalmani, V. Barone, B. Mennucci, G. A. Petersson, H. Nakatsuji, M. Caricato, X. Li, H. P. Hratchian, A. F. Izmaylov, J. Bloino, G. Zheng, J. L. Sonnenberg, M. Hada, M. Ehara, K. Toyota, R. Fukuda, J. Hasegawa, M. Ishida, T. Nakajima, Y. Honda, O. Kitao, H. Nakai, T. Vreven, Jr. J. A. Montgomery, J. E. Peralta, F. Ogliaro, M. Bearpark, J. J. Heyd, E. Brothers, K. N. Kudin, V. N. Staroverov, R. Kobayashi, J. Normand, K. Raghavachari, A. Rendell, J. C. Burant, S. S. Iyengar, J. Tomasi, M. Cossi, N. Rega, J. M. Millam, M. Klene, J. E. Knox, J. B. Cross, V. Bakken, C. Adamo, J. Jaramillo, R. Gomperts, R. E. Stratmann, O. Yazyev, A. J. Austin, R. Cammi, C. Pomelli, J. W. Ochterski, R. L. Martin, K. Morokuma, V. G. Zakrzewski, G. A. Voth, P. Salvador, J. J. Dannenberg, S. Dapprich, A. D. Daniels, O. Farkas, J. B. Foresman, J. V. Ortiz, J. Cioslowski, D. J. Fox, *Gaussian, Inc.*, Wallingford CT, **2013**.
2. E. F. C. Byrd, B. M. Rice, *J. Phys. Chem. A* **2006**, *110*, 1005-1013.

3. T. Lu, F. Chen, *J. Comput. Chem.* **2012**, *33*, 580.
4. H. D. B.Jenkins, D. Tudela, L. Glasser, *Inorg. Chem.* **2002**, *41*, 2364.
5. C. L. Mader, In Organic Energetic Compounds; Markinas, P. L., Ed.; Nova Science Publishers: Commack, New York, **1996**; p. 193.
6. S. Beaucamp, N. Marchet, D. Mathieu and V. Agafonov, *Acta Crystallographica Sec. B*, **59**, **2003**, 498-504.
7. C. M. Tarver, *J. Chem. Eng. Data*, **1979**, *24*, 136.
8. C. Ye and J. M. Shreeve, *J. Chem. Eng. Data*, **2008**, *53*, 520–524.
9. C. Ye and J. M. Shreeve, *J. Phys. Chem. A*, **2007**, *111*, 1456-1461.
10. B. M. Rice and D. M. Sorescu, *J. Phys. Chem. B*, **2004**, *108*, 17730-17739.
11. P. Politzer and J. S. Murray, *Cent. Eur. J. Energ. Mater.*, **2014**, *11*, 459-474.
12. M. J. Kamlet, S. J. Jabcobs, *J. Chem. Phys.* **1968**, *48*, 23.
13. P. Politzer, J. Martinez, J. S. Murray, M. C. Concha, A. Toro-Labbé, *Mol. Phys.* **2009**, *107*, 2095.
14. H. Muthurajan and A. H. Ghee, *Cent. Eur. J. Energ. Mater.*, **2008**, *5*, 19-35.
15. Iyer S, Slagg N (1988) In: Liebman JF, Greenberg A (eds) Structure and reactivity. VCH, New York, Ch 7.
16. Storm CB, Stine JR, Kramer JF (1990) In: Bulusu SN (ed) Chemistry and physics of energetic materials. Kluwer, Dordrecht, Ch 27.
17. Meyer R, Köhler J, Hornburg A (2007) Explosives, 6th edn. Wiley-VCH, Weinheim.
18. Sućeska M (1995) Test methods for explosives. Springer, New York.
19. Rice BM, Hare JJ (2002) *J Phys Chem A* **106**:1770–1783.

20. Dlott DD (2003) In: Politzer P, Murray JS (eds) Energetic materials, part 2. Detonation, combustion. Elsevier, Amsterdam, Ch 6.
21. Doherty RM, Watt DS (2008) Propellants Explos Pyrotech 33:4–13.
22. M. Pospíšil, P. Vávra, M. C. Concha, J. S. Murray, P. Politzer, J Mol Model (2011) 17:2569–2574.
23. Murray JS, Concha MC, Politzer P (2009) Mol Phys 107:89–97
24. Pospíšil M, Vávra P, Concha MC, Murray JS, Politzer P (2010) J Mol Model 16:895–901
25. Pospíšil M, Vávra P, Concha MC, Murray JS, Politzer P (2011) J Mol Model 17:2569–2574.

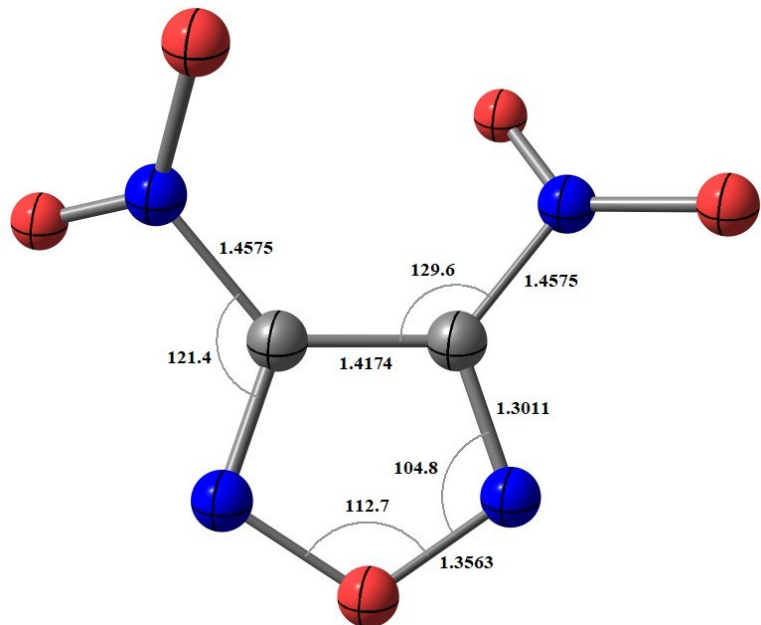


Figure S1. Selective bond lengths (\AA) and angles ($^\circ$) for **O1**.

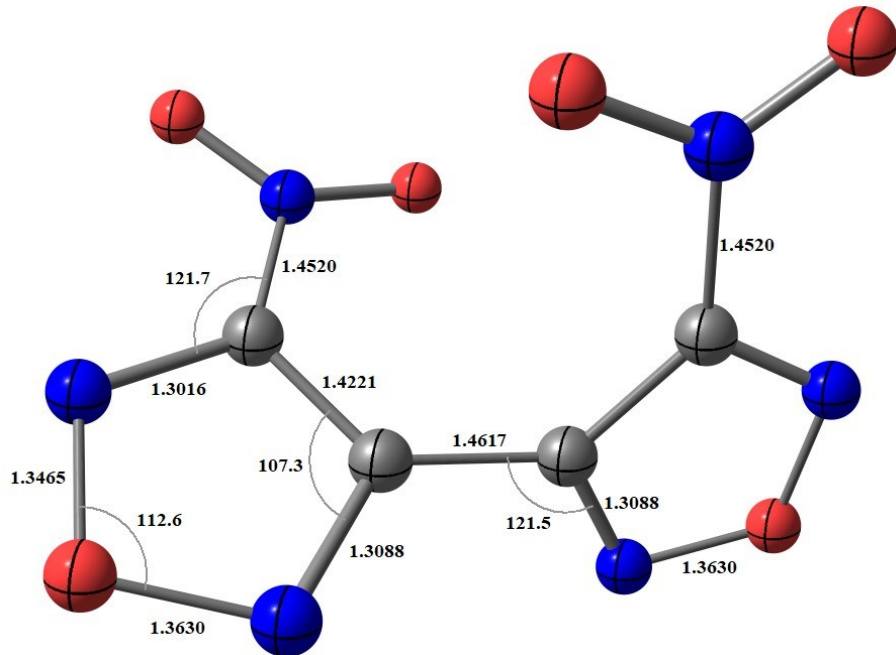


Figure S2. Selective bond lengths (\AA) and angles ($^{\circ}$) for **O2**.

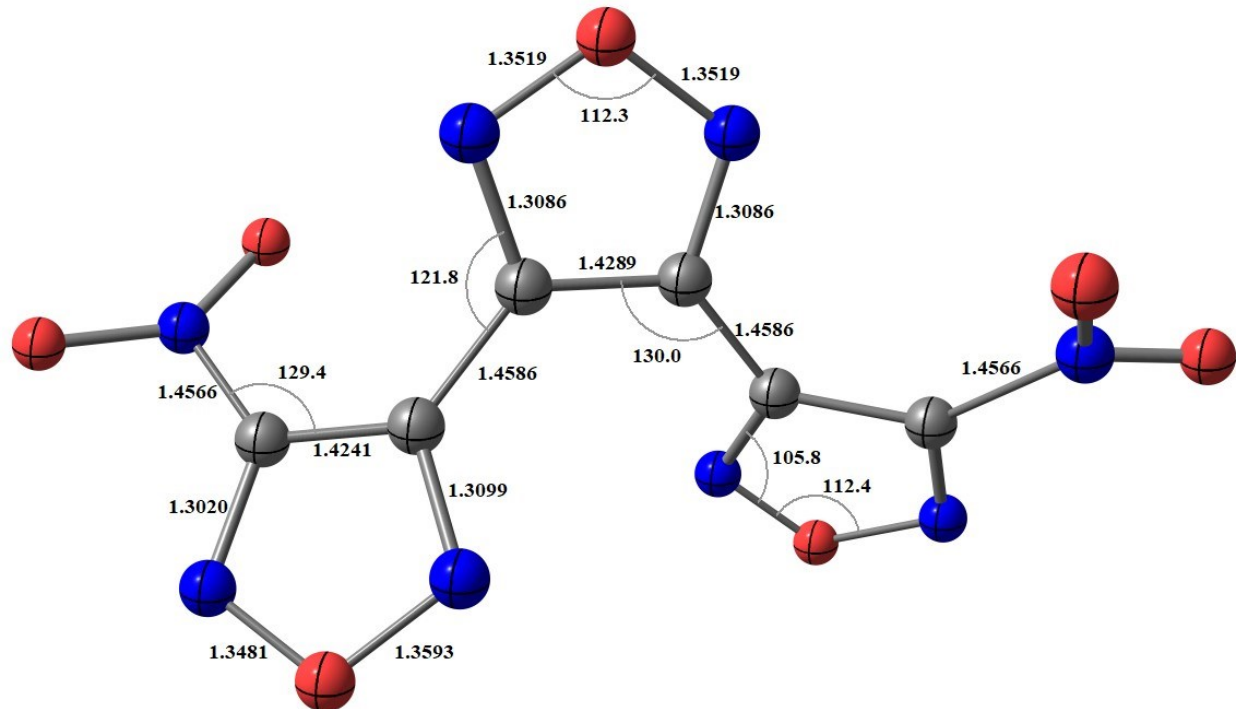


Figure S3. Selective bond lengths (\AA) and angles ($^{\circ}$) for **O3**.

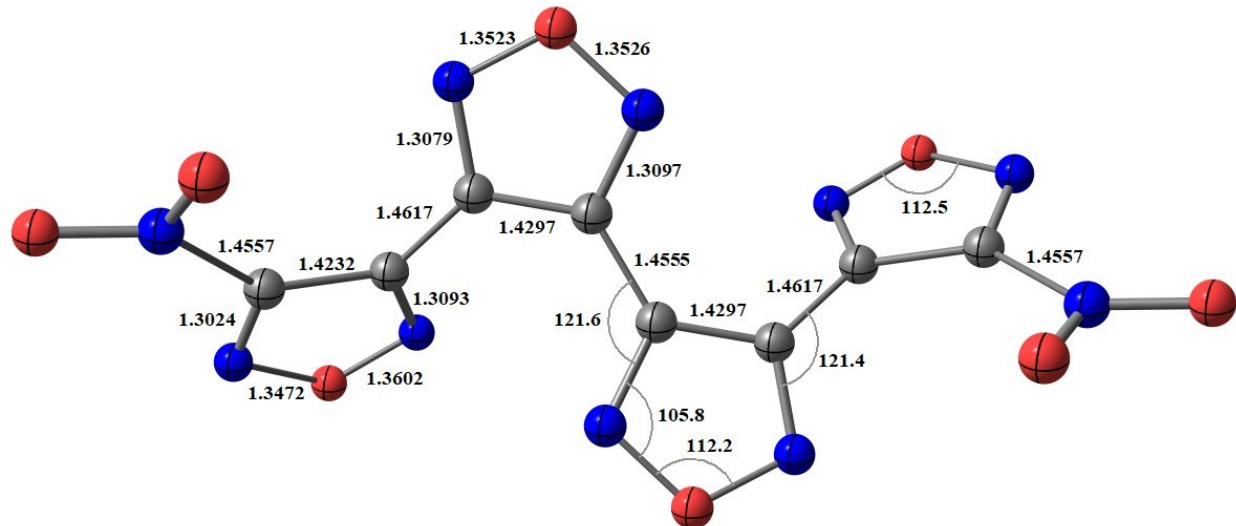


Figure S4. Selective bond lengths (\AA) and angles ($^\circ$) for **O4**.

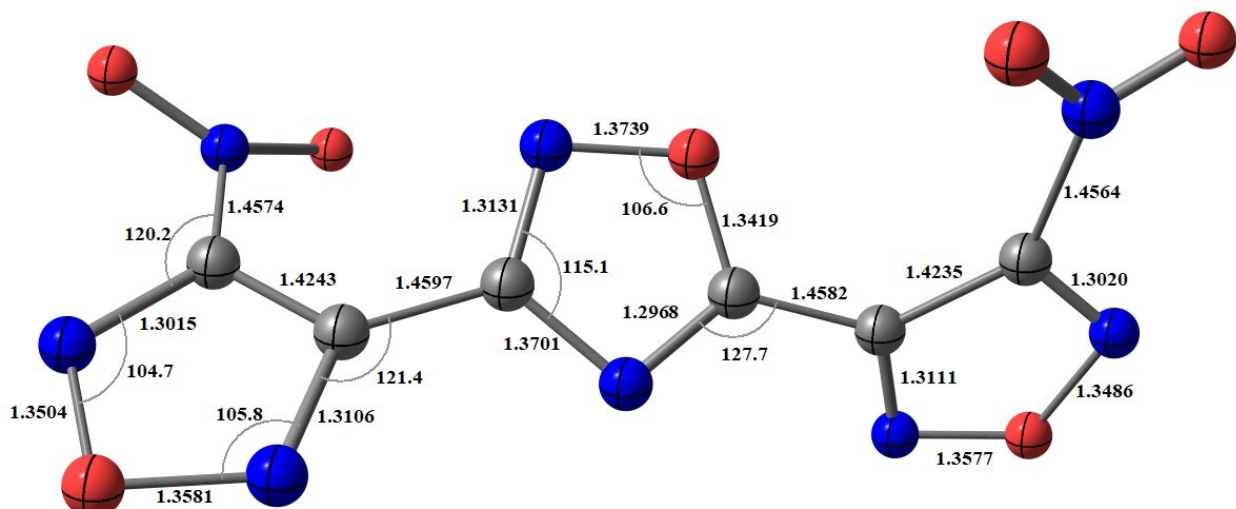


Figure S5. Selective bond lengths (\AA) and angles ($^\circ$) for **O5**.

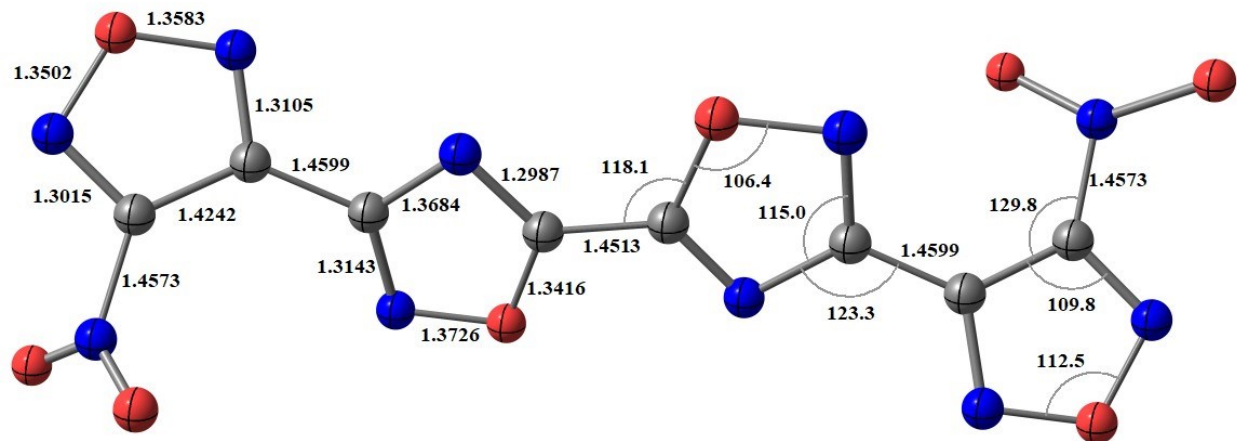


Figure S6. Selective bond lengths (\AA) and angles ($^{\circ}$) for **O6**.

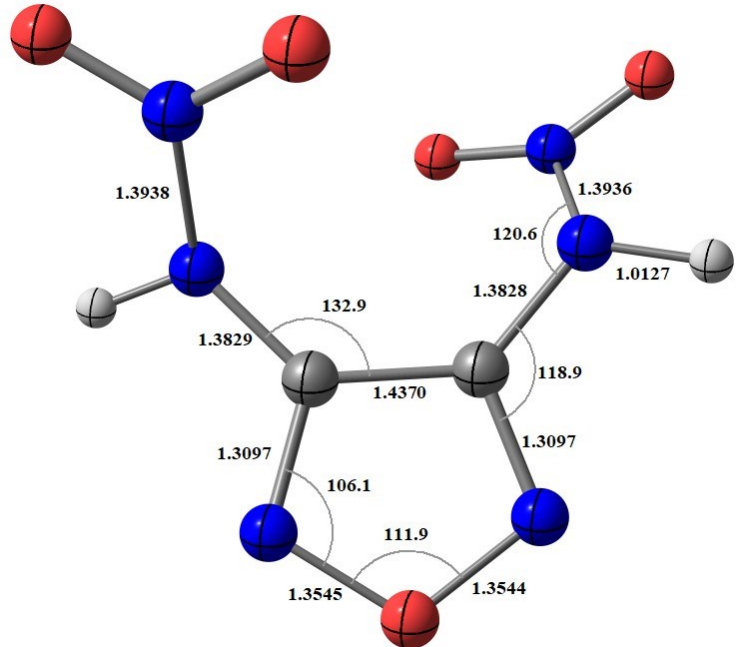


Figure S7. Selective bond lengths (\AA) and angles ($^{\circ}$) for **O7**.

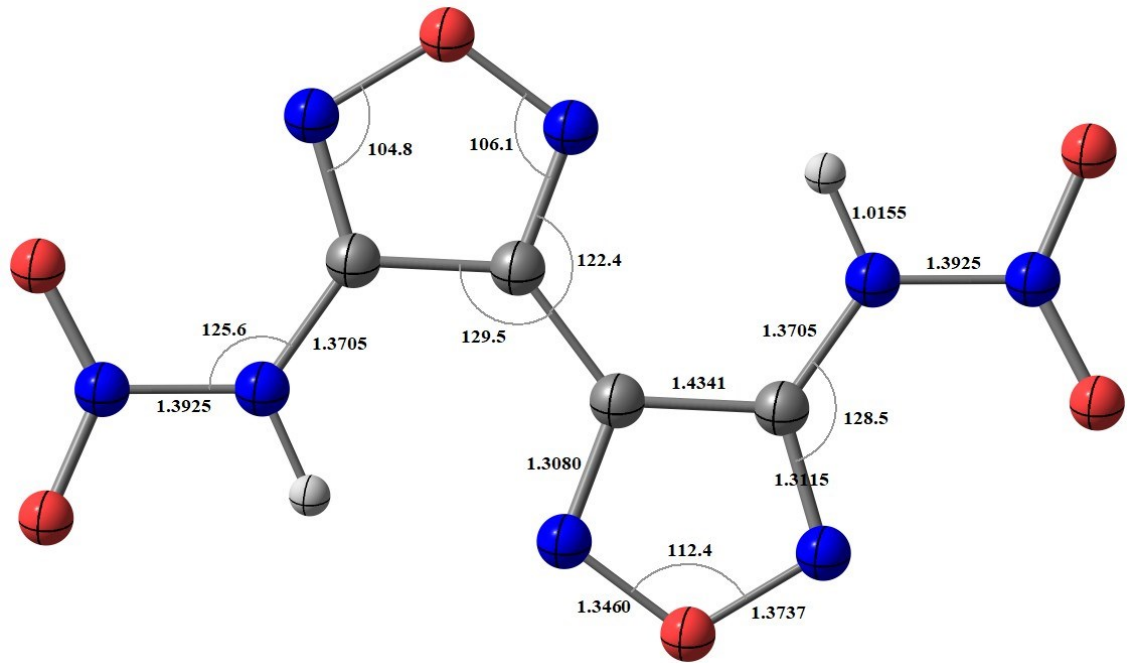


Figure S8. Selective bond lengths (\AA) and angles ($^\circ$) for **O8**.

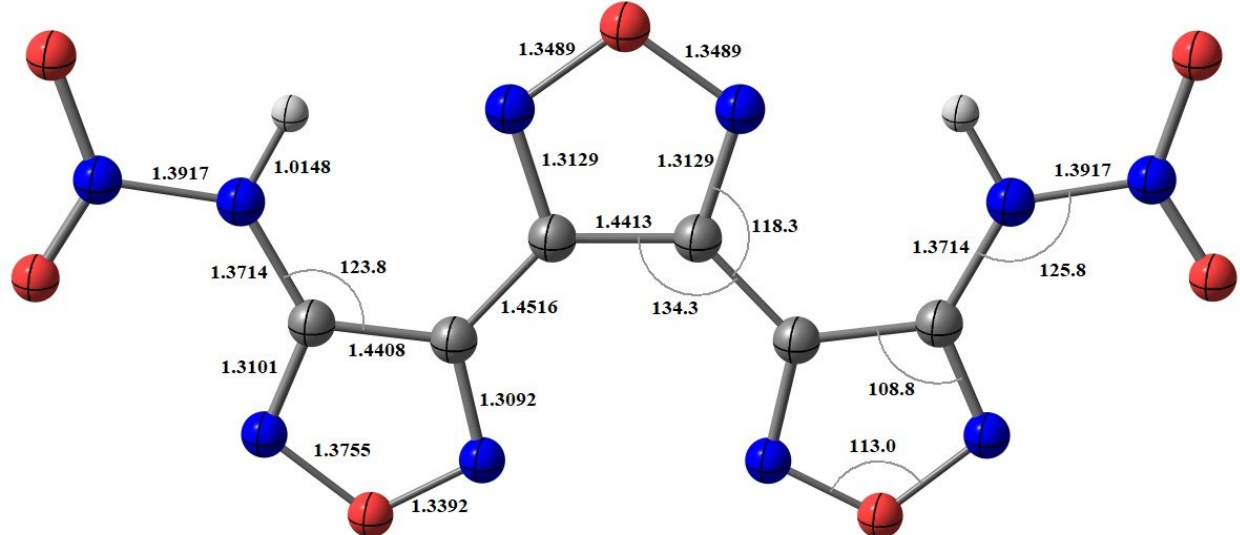


Figure S9. Selective bond lengths (\AA) and angles ($^\circ$) for **O9**.

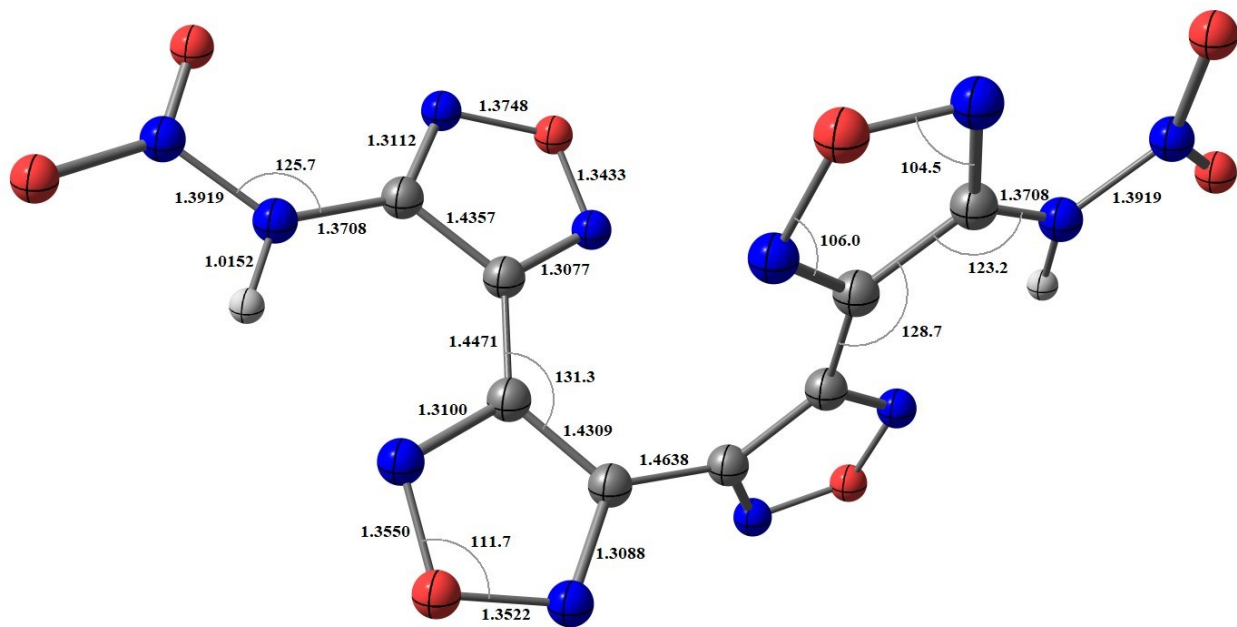


Figure S10. Selective bond lengths (\AA) and angles ($^{\circ}$) for **O10**.

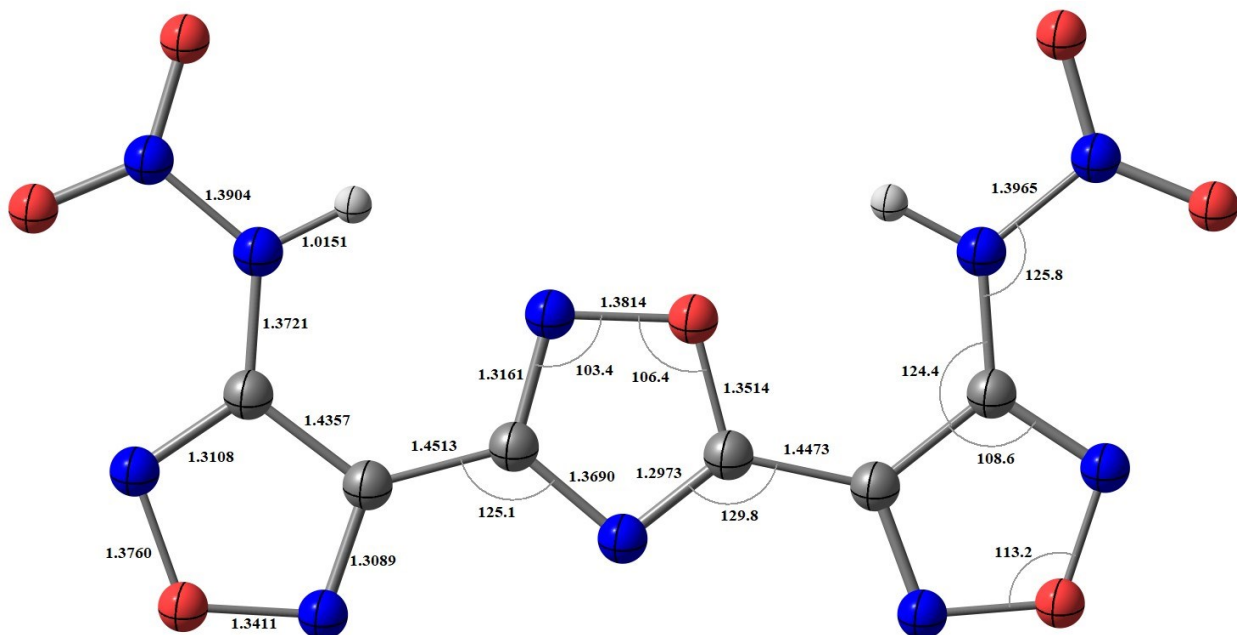


Figure S11. Selective bond lengths (\AA) and angles ($^{\circ}$) for **O11**.

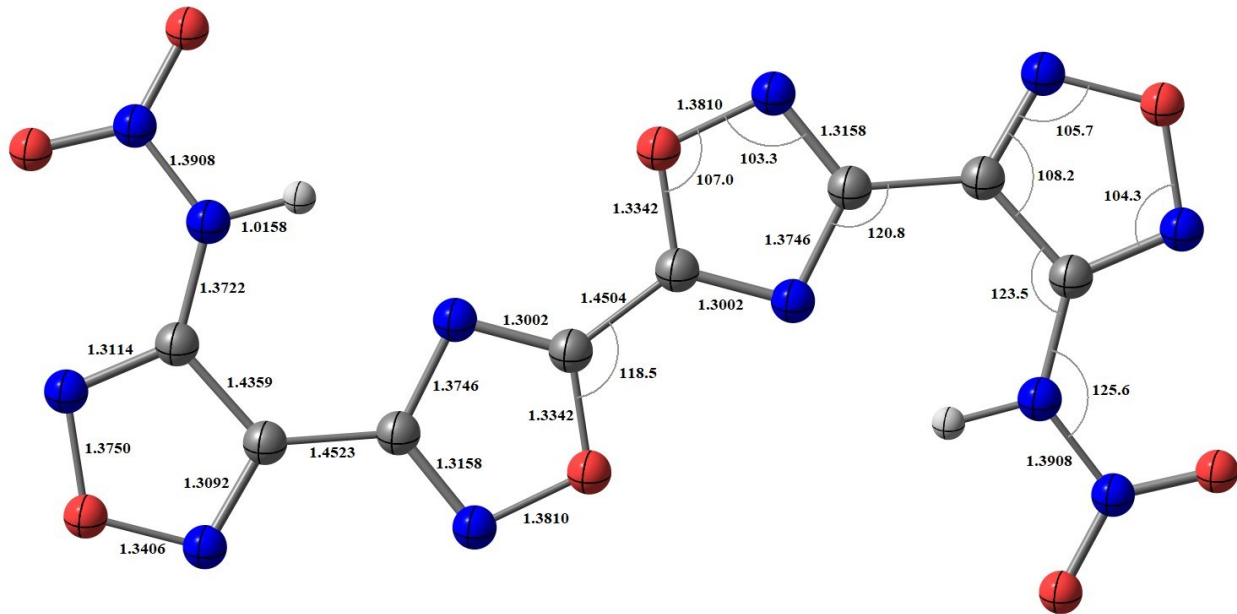


Figure S12. Selective bond lengths (\AA) and angles ($^{\circ}$) for **O12**.

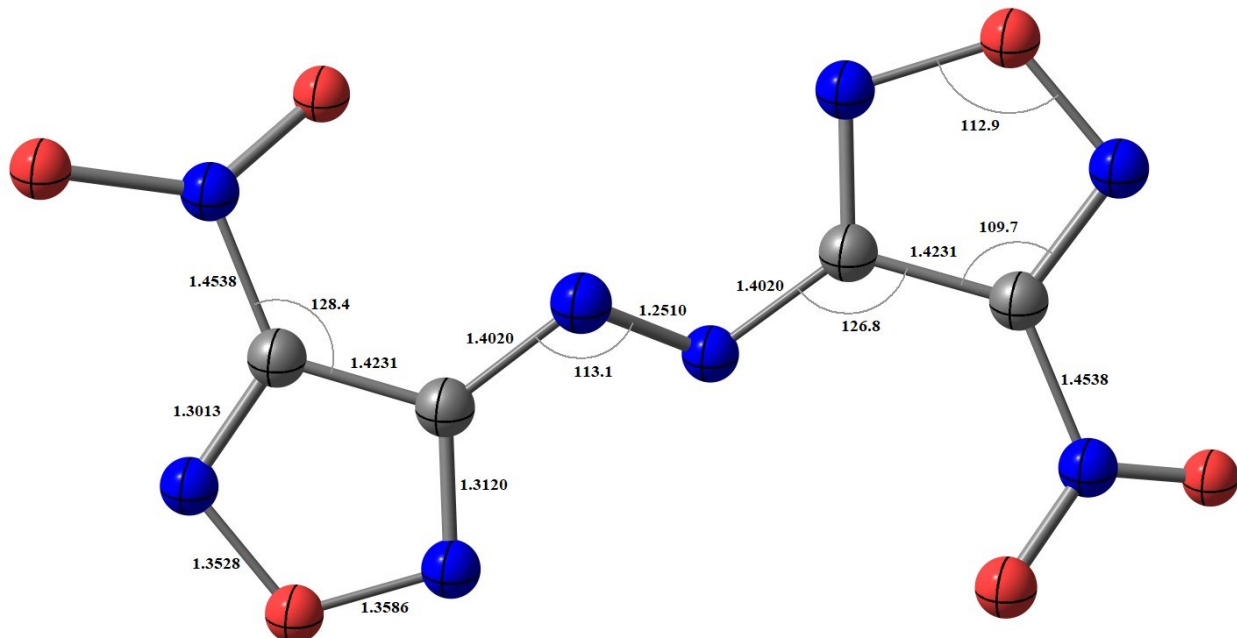


Figure S13. Selective bond lengths (\AA) and angles ($^{\circ}$) for **O13**.

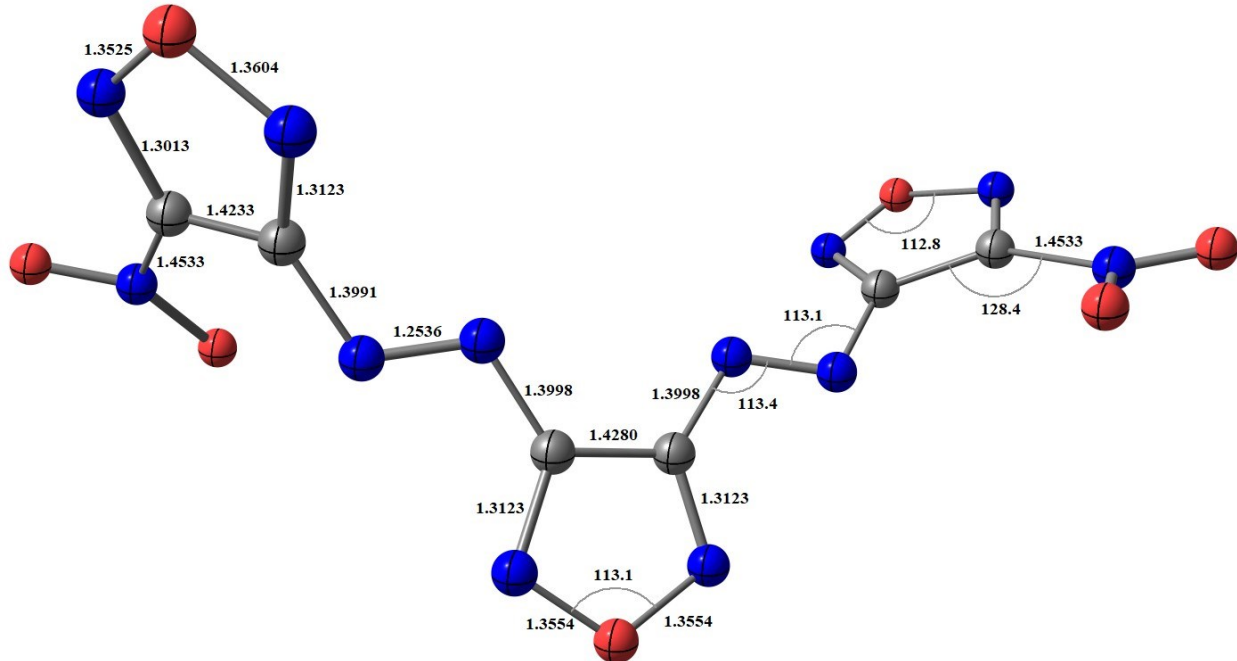


Figure S14. Selective bond lengths (\AA) and angles ($^{\circ}$) for **O14**.

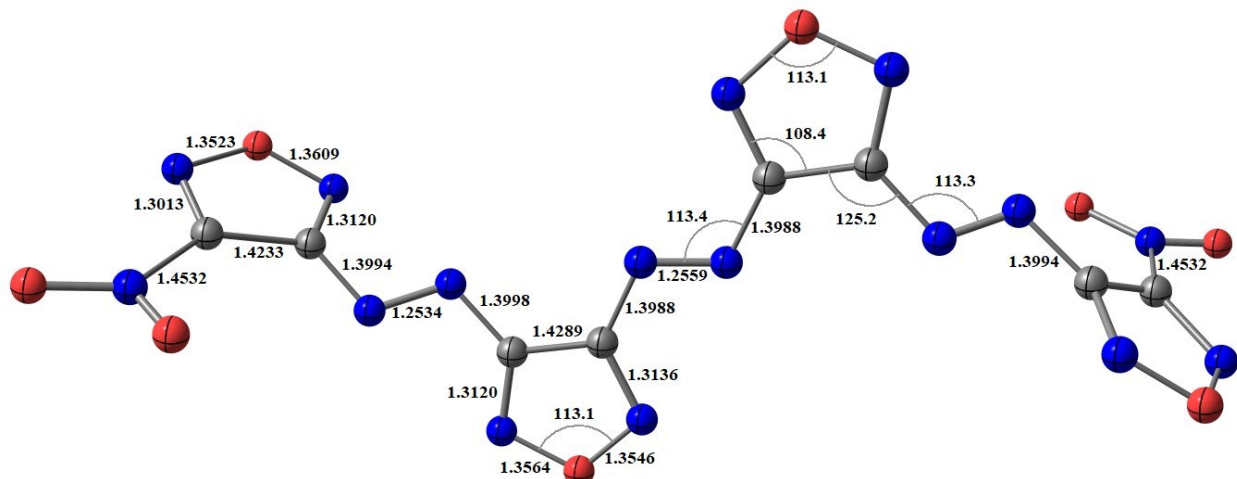


Figure S15. Selective bond lengths (\AA) and angles ($^{\circ}$) for **O15**.

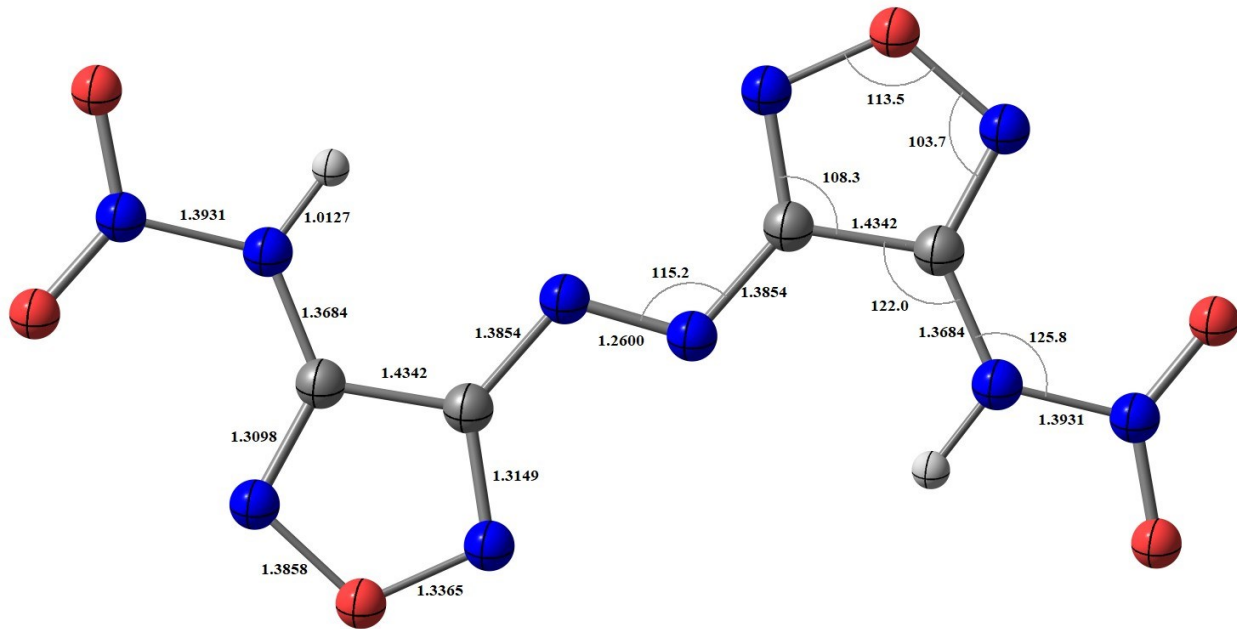


Figure S16. Selective bond lengths (\AA) and angles ($^{\circ}$) for **O16**.

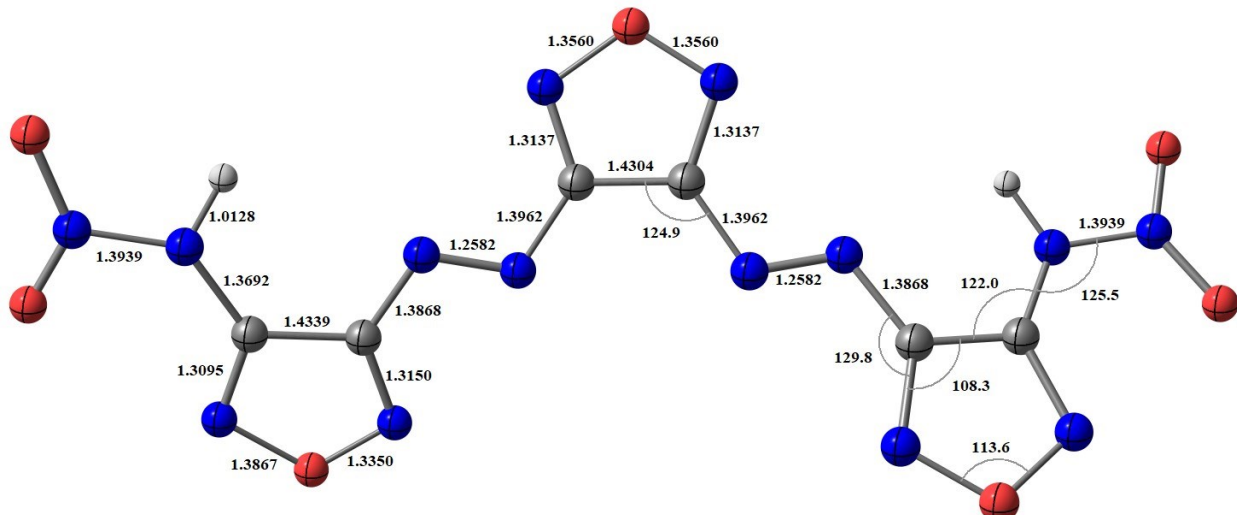


Figure S17. Selective bond lengths (\AA) and angles ($^{\circ}$) for **O17**.

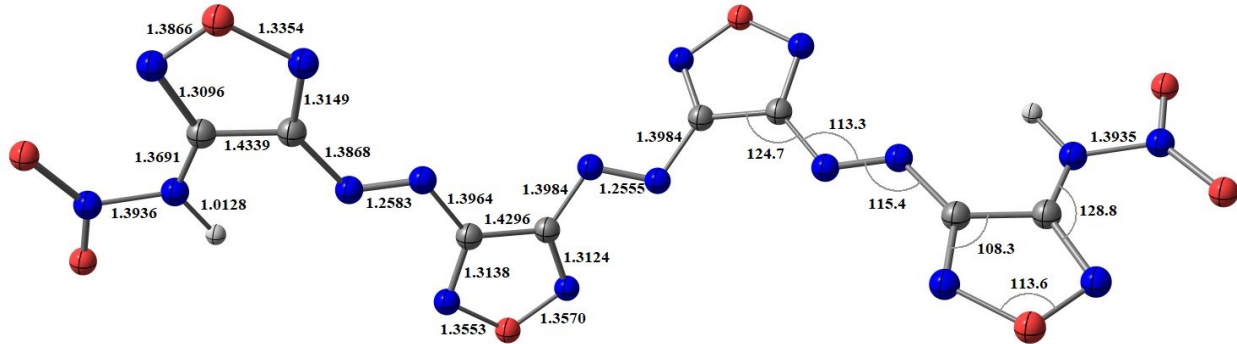
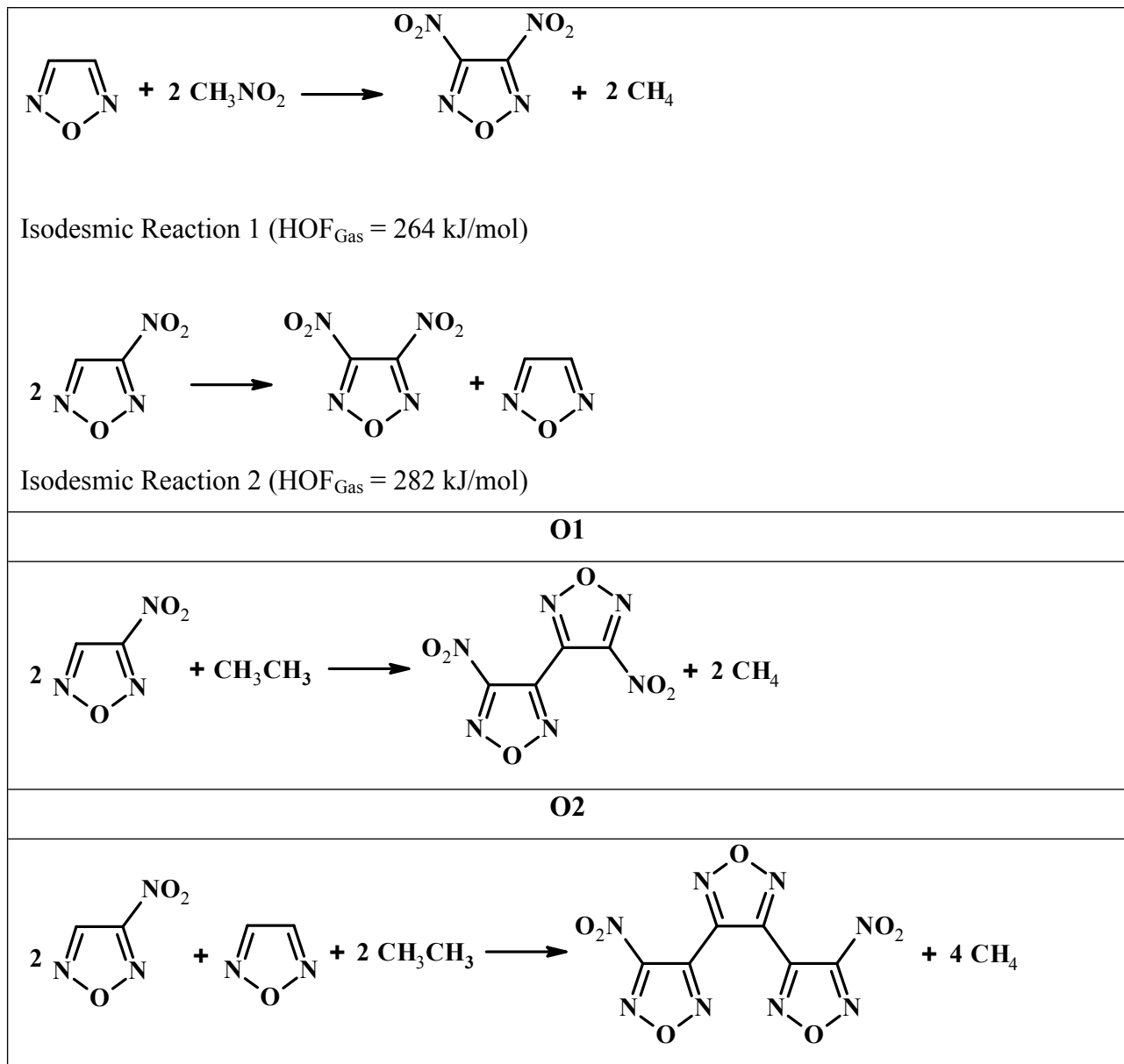
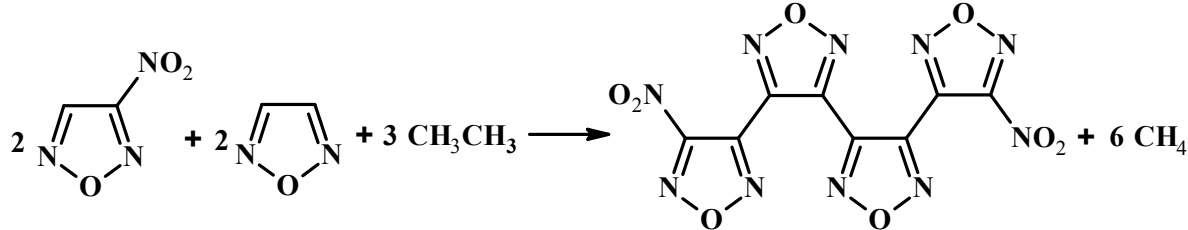


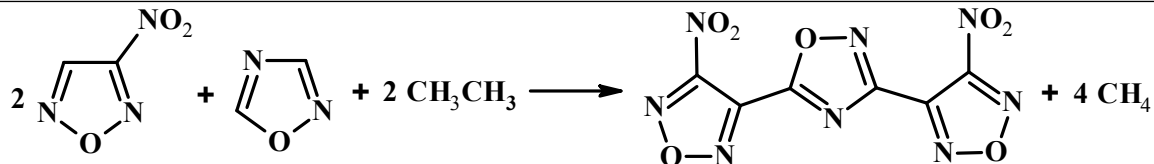
Figure S18. Selective bond lengths (\AA) and angles ($^{\circ}$) for **O18**.



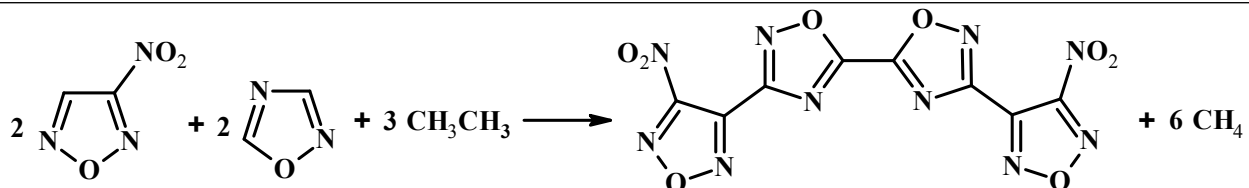
O3



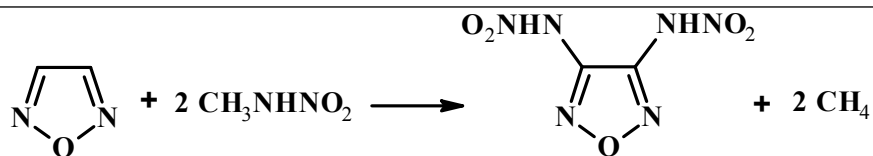
O4



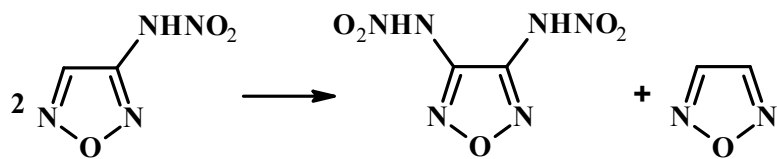
O5



O6

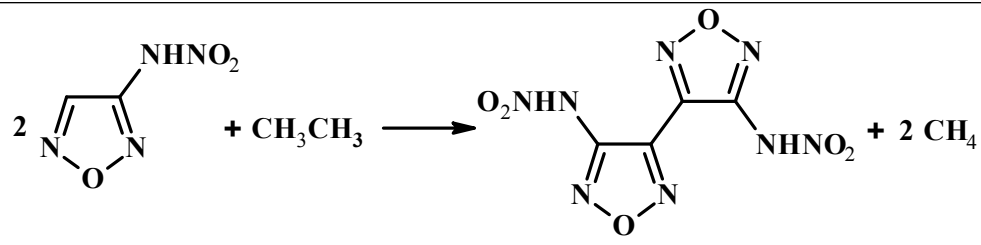


Isodesmic Reaction 1 ($\text{HOF}_{\text{Gas}} = 329 \text{ kJ/mol}$)

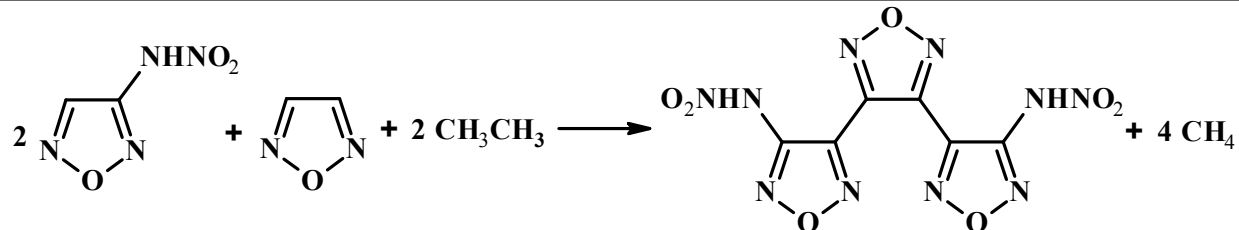


Isodesmic Reaction 2 ($\text{HOF}_{\text{Gas}} = 338 \text{ kJ/mol}$)

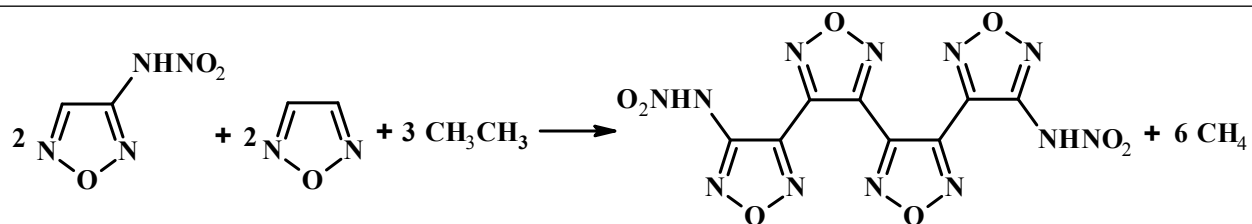
O7



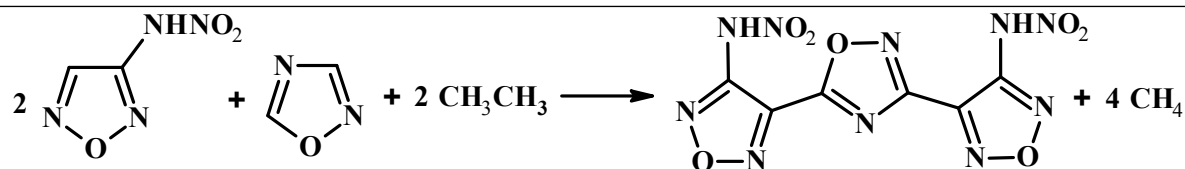
O8



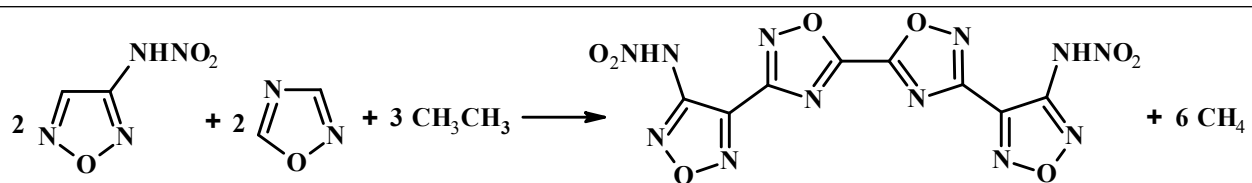
O9



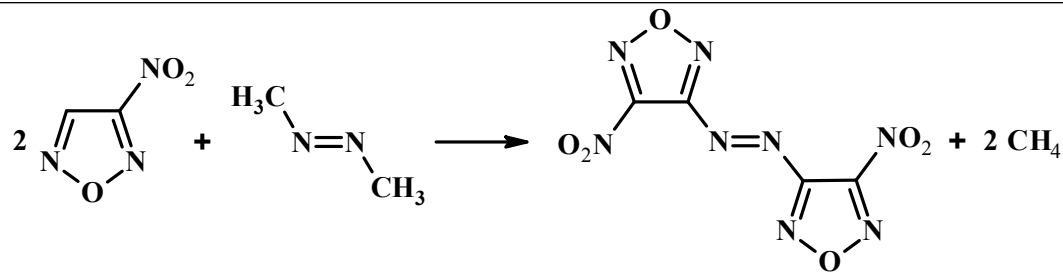
O10



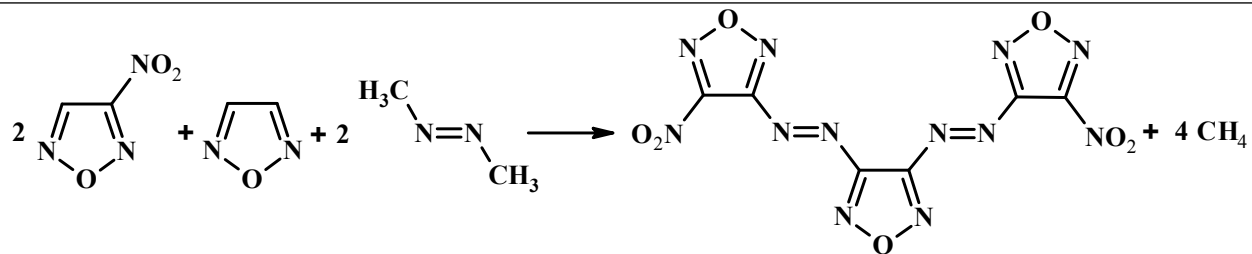
O11



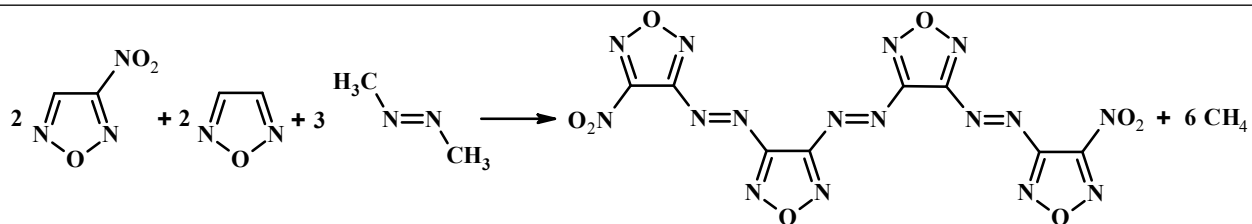
O12



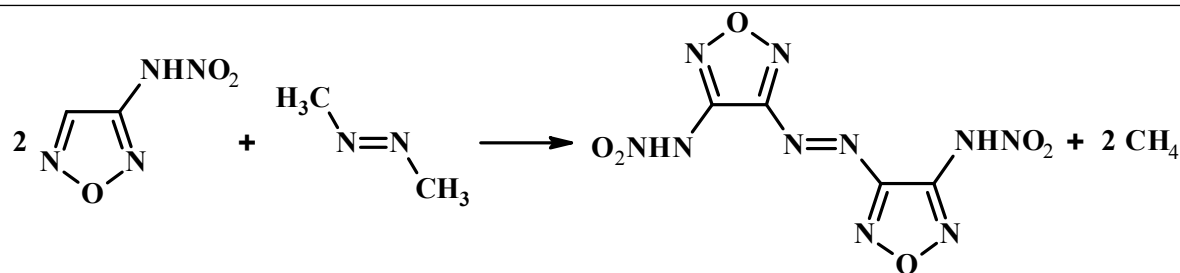
O13



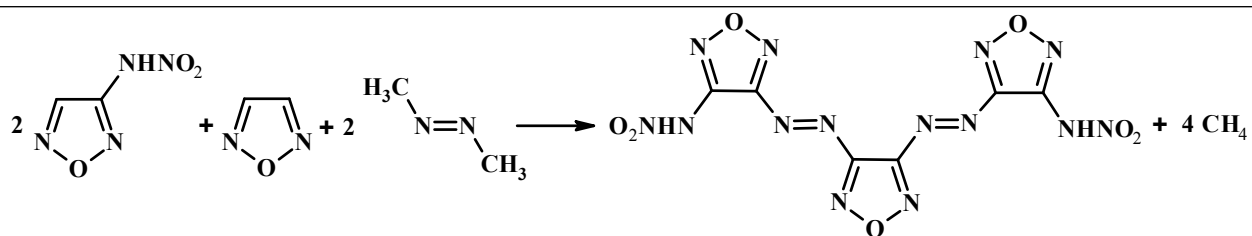
O14



O15



O16



O17

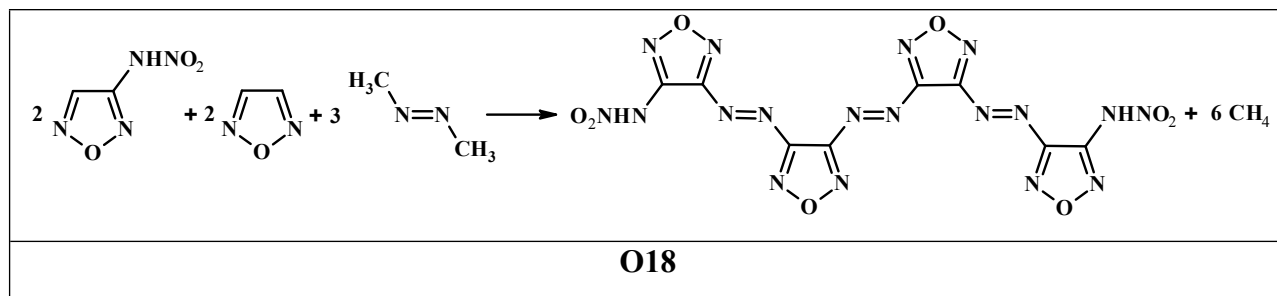


Figure S19. Isodesmic reaction schemes for oxadiazole derivatives.

Table S6. Optimized coordinates of **O1** form at B3PW91/6-31G(d,p) level of theory.

7	1.128337000	1.625703000	0.030963000
8	-0.000224000	2.377279000	0.000038000
6	0.708513000	0.394266000	0.014371000
7	-1.128635000	1.625514000	-0.030918000
6	-0.708604000	0.394144000	-0.014363000
7	1.635538000	-0.725197000	0.122834000
8	1.233562000	-1.655858000	0.801354000
8	2.703868000	-0.615802000	-0.444801000
7	-1.635409000	-0.725487000	-0.122859000
8	-2.704018000	-0.616059000	0.444243000
8	-1.232973000	-1.656335000	-0.800858000

Table S7. Optimized coordinates of **O2** form at B3PW91/6-31G(d,p) level of theory.

8	-2.575007000	-1.630449000	0.943576000
7	-1.256700000	-1.954703000	0.822307000
7	-2.870343000	-0.444014000	0.379380000
6	-0.710326000	-0.958972000	0.172053000
6	-1.738514000	-0.014672000	-0.098859000
6	0.710323000	-0.958974000	-0.172052000
6	1.738513000	-0.014674000	0.098859000
7	1.256697000	-1.954709000	-0.822300000
7	2.870341000	-0.444017000	-0.379380000
8	2.575002000	-1.630452000	-0.943580000
7	1.644799000	1.232896000	0.835794000
8	2.623554000	1.949058000	0.865136000
8	0.563655000	1.431724000	1.378358000
7	-1.644798000	1.232897000	-0.835802000
8	-2.623547000	1.949062000	-0.865135000
8	-0.563651000	1.431720000	-1.378355000

Table S8. Optimized coordinates of **O3** form at B3PW91/6-31G(d,p) level of theory.

7	3.337183000	-1.642603000	-0.736340000
8	2.225812000	-2.159403000	-1.297759000
6	2.959428000	-0.500322000	-0.238741000
7	1.149558000	-1.339479000	-1.167082000
6	1.574576000	-0.295283000	-0.500026000
6	0.687237000	0.821379000	-0.194790000
6	-0.687204000	0.821608000	0.195915000
7	1.078774000	2.064598000	-0.311392000
7	-1.078276000	2.064948000	0.312718000
8	0.000394000	2.817831000	0.000718000
6	-1.575007000	-0.294764000	0.500963000
7	-1.150805000	-1.338590000	1.169108000
6	-2.959598000	-0.499805000	0.238330000
8	-2.227307000	-2.158307000	1.299156000
7	-3.338015000	-1.641734000	0.736244000
7	-3.887268000	0.323106000	-0.525814000
8	-3.373393000	1.014369000	-1.392060000
8	-5.067398000	0.235239000	-0.248776000
7	3.888022000	0.322896000	0.523955000
8	5.067763000	0.235252000	0.245199000
8	3.375279000	1.013908000	1.391060000

Table S9. Optimized coordinates of **O4** form at B3PW91/6-31G(d,p) level of theory.

7	4.779742000	1.152387000	-0.706137000
6	4.134799000	0.240678000	-0.036072000
8	3.927445000	1.531832000	-1.678086000
6	2.846319000	0.043655000	-0.607345000
7	2.748964000	0.854310000	-1.630840000
6	1.764773000	-0.874203000	-0.254642000
7	1.976711000	-2.157763000	-0.120126000
6	0.371810000	-0.625706000	-0.049553000
8	0.770588000	-2.700974000	0.160966000
7	-0.210160000	-1.770642000	0.206836000
6	-0.371739000	0.625549000	-0.049649000
6	-1.764707000	0.874034000	-0.254720000
7	0.210263000	1.770520000	0.206514000
7	-1.976611000	2.157626000	-0.120435000
8	-0.770469000	2.700865000	0.160514000
6	-2.846285000	-0.043856000	-0.607228000
7	-2.748873000	-0.854868000	-1.630437000

6	-4.134846000	-0.240595000	-0.036034000
8	-3.927423000	-1.532269000	-1.677632000
7	-4.779813000	-1.152414000	-0.705925000
7	4.716147000	-0.372204000	1.149452000
8	3.909149000	-0.839096000	1.939975000
8	5.927032000	-0.353109000	1.251450000
7	-4.716274000	0.372678000	1.149251000
8	-3.909321000	0.839583000	1.939809000
8	-5.927179000	0.353826000	1.251054000

Table S10. Optimized coordinates of **O5** form at B3PW91/6-31G(d,p) level of theory.

7	4.607442000	-0.747503000	-0.566496000
6	3.633593000	-0.041493000	-0.069398000
8	3.999630000	-1.781466000	-1.187022000
6	2.384867000	-0.646785000	-0.390150000
7	2.646129000	-1.721973000	-1.092549000
6	1.012462000	-0.235569000	-0.110743000
7	0.690543000	1.026780000	0.053770000
7	-0.034820000	-1.116026000	-0.038709000
8	-0.667420000	0.982541000	0.257396000
6	-1.024670000	-0.308937000	0.185796000
6	-2.423669000	-0.654468000	0.408628000
6	-3.632081000	-0.007432000	0.024621000
7	-2.754034000	-1.721079000	1.095825000
7	-4.652558000	-0.683372000	0.468376000
8	-4.111466000	-1.733234000	1.119226000
7	3.920715000	1.124383000	0.756657000
8	3.180711000	1.275011000	1.715983000
8	4.867807000	1.814755000	0.433075000
7	-3.820584000	1.171333000	-0.809768000
8	-4.866928000	1.777206000	-0.693233000
8	-2.892689000	1.420225000	-1.565707000

Table S11. Optimized coordinates of **O6** form at B3PW91/6-31G(d,p) level of theory.

7	-6.303239000	1.065994000	0.056649000
6	-5.382345000	0.146683000	0.028355000
8	-5.627198000	2.231953000	-0.024045000
6	-4.097918000	0.752904000	-0.076520000
7	-4.284298000	2.049525000	-0.115116000
6	-2.762500000	0.173455000	-0.186454000

7	-2.564928000	-1.009554000	-0.723836000
7	-1.627438000	0.819783000	0.221475000
8	-1.202547000	-1.165497000	-0.663377000
6	-0.717427000	-0.050703000	-0.096061000
6	0.717492000	0.050641000	0.096261000
7	1.627496000	-0.819891000	-0.221181000
8	1.202627000	1.165502000	0.663429000
6	2.762553000	-0.173557000	0.186733000
7	2.565001000	1.009533000	0.723947000
6	4.097992000	-0.752979000	0.076907000
7	4.284545000	-2.049544000	0.116272000
6	5.382320000	-0.146638000	-0.028456000
8	5.627444000	-2.231861000	0.024773000
7	6.303305000	-1.065851000	-0.056839000
7	5.740117000	1.257138000	-0.186901000
8	4.956506000	1.919741000	-0.848536000
8	6.778127000	1.627418000	0.326349000
7	-5.740355000	-1.257109000	0.186185000
8	-4.957200000	-1.919969000	0.848095000
8	-6.778061000	-1.627164000	-0.327837000

Table S12. Optimized coordinates of **O7** form at B3PW91/6-31G(d,p) level of theory.

7	-2.232204000	-1.025344000	0.319146000
8	-2.965343000	0.067901000	-0.000178000
6	-0.977877000	-0.667367000	0.201915000
7	-2.182901000	1.126308000	-0.319340000
6	-0.946271000	0.711484000	-0.201621000
7	0.009877000	-1.562962000	0.568717000
7	0.081562000	1.560763000	-0.568421000
7	1.178927000	1.750853000	0.269355000
8	1.878773000	2.703095000	-0.013166000
8	1.332267000	0.936011000	1.159932000
7	1.097403000	-1.802942000	-0.269354000
8	1.288228000	-0.995381000	-1.159273000
8	1.752522000	-2.786653000	0.012506000
1	-0.263160000	-2.399950000	1.069213000
1	-0.152180000	2.408734000	-1.070275000

Table S13. Optimized coordinates of **O8** form at B3PW91/6-31G(d,p) level of theory.

8	1.039875000	-2.611006000	-0.000590000
---	-------------	--------------	--------------

7	-0.034900000	-1.800793000	-0.000637000
7	2.221986000	-1.911270000	-0.000865000
6	0.431084000	-0.578661000	-0.000883000
6	1.863437000	-0.649779000	-0.001006000
6	-0.431084000	0.578662000	-0.000852000
6	-1.863436000	0.649779000	-0.000949000
7	0.034899000	1.800794000	-0.000552000
7	-2.221987000	1.911270000	-0.000766000
8	-1.039876000	2.611006000	-0.000467000
7	2.661495000	0.464393000	-0.001601000
7	-2.661494000	-0.464393000	-0.001571000
7	-4.054035000	-0.464013000	0.001028000
8	-4.609417000	0.612737000	0.001710000
8	-4.545292000	-1.578853000	0.002051000
7	4.054035000	0.464013000	0.000976000
8	4.609417000	-0.612737000	0.001640000
8	4.545292000	1.578853000	0.002058000
1	2.250385000	1.392996000	-0.000582000
1	-2.250383000	-1.392996000	-0.000585000

Table S14. Optimized coordinates of **O9** form at B3PW91/6-31G(d,p) level of theory.

7	3.733171000	-1.679668000	0.013671000
8	2.679932000	-2.564388000	0.010352000
6	3.165692000	-0.498853000	0.011171000
7	1.486407000	-1.957066000	0.006683000
6	1.735308000	-0.671732000	0.006862000
7	3.786211000	0.724088000	0.015535000
7	5.160943000	0.939952000	-0.005990000
8	5.882427000	-0.032772000	-0.012861000
8	5.469626000	2.119838000	-0.013678000
6	0.720636000	0.366267000	0.002971000
6	-0.720637000	0.366267000	-0.002985000
7	1.111221000	1.619714000	0.004599000
7	-1.111226000	1.619713000	-0.004623000
8	-0.000003000	2.384309000	-0.000014000
6	-1.735308000	-0.671734000	-0.006872000
7	-1.486408000	-1.957068000	-0.006685000
6	-3.165690000	-0.498853000	-0.011190000
8	-2.679936000	-2.564386000	-0.010350000
7	-3.733172000	-1.679664000	-0.013671000

7	-3.786209000	0.724091000	-0.015573000
7	-5.160942000	0.939953000	0.005927000
8	-5.469625000	2.119838000	0.013747000
8	-5.882420000	-0.032776000	0.012954000
1	3.238132000	1.578101000	0.008971000
1	-3.238124000	1.578099000	-0.009019000

Table S15. Optimized coordinates of **O10** form at B3PW91/6-31G(d,p) level of theory.

7	2.725576000	1.825895000	1.471868000
6	3.010711000	0.854524000	0.638630000
8	1.451435000	1.544948000	1.905045000
6	1.885865000	-0.034534000	0.564382000
7	0.952512000	0.424566000	1.356997000
6	1.741152000	-1.246892000	-0.212367000
7	2.722594000	-1.684571000	-0.961499000
6	0.657369000	-2.174770000	-0.321763000
8	2.283193000	-2.837325000	-1.521863000
7	1.024360000	-3.137032000	-1.129459000
6	-0.657445000	-2.174769000	0.321586000
6	-1.741143000	-1.246770000	0.212367000
7	-1.024513000	-3.137135000	1.129124000
7	-2.722638000	-1.684519000	0.961390000
8	-2.283341000	-2.837419000	1.521534000
6	-1.885744000	-0.034248000	-0.564146000
7	-0.952330000	0.424948000	-1.356634000
6	-3.010564000	0.854850000	-0.638335000
8	-1.451111000	1.545534000	-1.904390000
7	-2.725255000	1.826476000	-1.471215000
7	4.168781000	0.659317000	-0.068452000
7	-4.168723000	0.659506000	0.068562000
7	5.275246000	1.503747000	-0.063387000
8	6.181030000	1.129002000	-0.787834000
8	5.222702000	2.488574000	0.640181000
7	-5.275430000	1.503614000	0.063048000
8	-6.181373000	1.128641000	0.787178000
8	-5.222831000	2.488529000	-0.640393000
1	4.266977000	-0.140935000	-0.685423000
1	-4.267071000	-0.140959000	0.685231000

Table S16. Optimized coordinates of **O11** form at B3PW91/6-31G(d,p) level of theory.

7	4.666938000	-1.019188000	-0.033122000
8	4.226188000	-2.320874000	-0.024486000
6	3.567968000	-0.303011000	-0.027698000
7	2.894078000	-2.425099000	-0.016734000
6	2.440817000	-1.194145000	-0.018179000
6	1.025409000	-0.892194000	-0.009556000
8	0.685992000	0.415884000	-0.012820000
7	0.004775000	-1.693005000	0.001517000
7	-0.694671000	0.460305000	-0.002577000
6	-1.040901000	-0.809394000	0.005441000
6	-2.444833000	-1.176896000	0.016834000
7	-2.870635000	-2.414606000	0.025479000
6	-3.588901000	-0.309602000	0.019473000
8	-4.209551000	-2.338010000	0.032975000
7	-4.675128000	-1.043174000	0.030302000
7	-3.496442000	1.059392000	0.016497000
7	-4.565604000	1.947488000	-0.021142000
8	-5.683100000	1.479830000	-0.026478000
8	-4.228216000	3.119608000	-0.042146000
7	3.474476000	1.065939000	-0.039679000
7	4.546935000	1.957882000	0.026280000
8	5.662631000	1.490671000	0.047576000
8	4.203512000	3.126849000	0.049688000
1	-2.588679000	1.513448000	0.001553000
1	2.578633000	1.534808000	-0.021673000

Table S17. Optimized coordinates of **O12** form at B3PW91/6-31G(d,p) level of theory.

7	-6.060446000	-0.888465000	0.032848000
8	-5.850231000	-2.247295000	0.027421000
6	-4.854519000	-0.373226000	0.036213000
7	-4.550841000	-2.577112000	0.032431000
6	-3.896709000	-1.443040000	0.037469000
7	-4.507926000	0.954287000	0.056185000
7	-5.385570000	2.023000000	-0.091859000
8	-6.569528000	1.772878000	-0.151362000
8	-4.832016000	3.109078000	-0.135064000
1	-3.527880000	1.220633000	0.034437000
6	-2.448431000	-1.335288000	0.039929000
7	-1.834405000	-0.105463000	0.038948000
7	-1.619022000	-2.356762000	0.042075000

6	-0.577579000	-0.438538000	0.040376000
8	-0.374932000	-1.757285000	0.042310000
6	0.577578000	0.438542000	0.040397000
8	0.374932000	1.757289000	0.042442000
7	1.834404000	0.105466000	0.038913000
7	1.619021000	2.356766000	0.042224000
6	2.448430000	1.335292000	0.039978000
6	3.896708000	1.443043000	0.037494000
6	4.854517000	0.373226000	0.036159000
7	4.550842000	2.577113000	0.032506000
7	6.060445000	0.888463000	0.032789000
8	5.850231000	2.247294000	0.027446000
7	4.507920000	-0.954286000	0.056054000
7	5.385570000	-2.023003000	-0.091904000
8	6.569536000	-1.772889000	-0.151292000
8	4.832019000	-3.109084000	-0.135063000
1	3.527875000	-1.220633000	0.034313000

Table S18. Optimized coordinates of **O13** form at B3PW91/6-31G(d,p) level of theory.

7	0.521223000	-0.204677000	-0.279185000
7	-0.521188000	0.204574000	0.278451000
6	-1.628275000	-0.625112000	0.051128000
6	-2.994737000	-0.230385000	0.004527000
7	-1.591455000	-1.935651000	0.000894000
7	-3.752789000	-1.283208000	-0.097311000
8	-2.889844000	-2.325017000	-0.089998000
6	1.628291000	0.625055000	-0.051920000
6	2.994738000	0.230373000	-0.004556000
7	1.591414000	1.935619000	-0.002537000
7	3.752721000	1.283283000	0.096968000
8	2.889803000	2.325054000	0.088655000
7	-3.545415000	1.114938000	-0.013516000
8	-4.715304000	1.245617000	0.291976000
8	-2.757326000	1.988631000	-0.345155000
7	3.545398000	-1.114939000	0.014532000
8	4.715659000	-1.245721000	-0.289484000
8	2.757080000	-1.988459000	0.346111000

Table S19. Optimized coordinates of **O14** form at B3PW91/6-31G(d,p) level of theory.

7	2.688701000	0.641427000	0.306455000
---	-------------	-------------	-------------

7	1.455611000	0.458681000	0.439115000
6	3.452182000	-0.463607000	0.698228000
6	4.706159000	-0.871294000	0.162423000
7	3.203203000	-1.218087000	1.742684000
7	5.180568000	-1.863188000	0.858399000
8	4.262317000	-2.067454000	1.830142000
6	0.693165000	1.601645000	0.171189000
6	-0.693181000	1.601588000	-0.171376000
7	1.092722000	2.845904000	0.291118000
7	-1.092789000	2.845815000	-0.291492000
8	-0.000051000	3.592915000	-0.000243000
7	-1.455569000	0.458550000	-0.439129000
7	-2.688675000	0.641271000	-0.306553000
6	-3.452108000	-0.463865000	-0.698118000
7	-3.203002000	-1.218692000	-1.742293000
6	-4.706139000	-0.871390000	-0.162308000
8	-4.262084000	-2.068102000	-1.829576000
7	-5.180449000	-1.863541000	-0.857985000
7	5.388534000	-0.370039000	-1.018710000
8	6.579398000	-0.596506000	-1.117041000
8	4.676223000	0.235054000	-1.807126000
7	-5.388664000	-0.369780000	1.018590000
8	-4.676457000	0.235572000	1.806900000
8	-6.579575000	-0.596067000	1.116742000

Table S20. Optimized coordinates of **O15** form at B3PW91/6-31G(d,p) level of theory.

7	-4.727132000	-0.724853000	-0.466823000
7	-3.554691000	-0.330031000	-0.668221000
6	-5.681632000	0.285849000	-0.627499000
6	-6.914615000	0.418545000	0.071003000
7	-5.662260000	1.194331000	-1.573924000
7	-7.602385000	1.401580000	-0.433001000
8	-6.837251000	1.868847000	-1.445340000
6	-2.609583000	-1.362233000	-0.640922000
6	-1.215998000	-1.196762000	-0.372078000
7	-2.829486000	-2.615858000	-0.959409000
7	-0.628359000	-2.364581000	-0.500079000
8	-1.616659000	-3.215851000	-0.865436000
7	-0.626341000	0.001629000	0.043481000
7	0.626381000	-0.000926000	-0.046429000

6	1.216007000	1.197518000	0.369002000
7	0.628513000	2.365541000	0.495764000
6	2.609424000	1.362878000	0.638779000
8	1.616699000	3.216825000	0.861460000
7	2.829302000	2.616623000	0.956809000
7	3.554300000	0.330493000	0.667378000
7	4.727005000	0.724972000	0.466856000
6	5.681147000	-0.285868000	0.628798000
6	6.914693000	-0.419172000	-0.068592000
7	5.660727000	-1.193933000	1.575598000
7	7.601798000	-1.402148000	0.436420000
8	6.835682000	-1.868775000	1.448300000
7	7.383375000	0.327365000	-1.223892000
8	8.575434000	0.301009000	-1.463275000
8	6.509682000	0.911796000	-1.848715000
7	-7.382189000	-0.328641000	1.226335000
8	-8.574066000	-0.302711000	1.466641000
8	-6.507844000	-0.913074000	1.850242000

Table S21. Optimized coordinates of **O16** form at B3PW91/6-31G(d,p) level of theory.

7	-0.605345000	-0.174217000	-0.011524000
7	0.605345000	0.174212000	0.011681000
6	1.518570000	-0.867577000	0.011130000
6	2.934127000	-0.639684000	0.044777000
7	1.310504000	-2.165458000	-0.023419000
7	3.556073000	-1.792345000	0.032155000
8	2.526860000	-2.719214000	-0.013099000
6	-1.518568000	0.867573000	-0.011116000
6	-2.934125000	0.639680000	-0.044782000
7	-1.310502000	2.165457000	0.023359000
7	-3.556070000	1.792343000	-0.032235000
8	-2.526855000	2.719216000	0.012896000
7	-3.464112000	-0.620708000	-0.099958000
7	3.464114000	0.620701000	0.100050000
7	4.815756000	0.940733000	-0.007075000
8	5.600188000	0.019094000	-0.055311000
8	5.037646000	2.138495000	-0.029207000
7	-4.815760000	-0.940729000	0.007117000
8	-5.600192000	-0.019085000	0.055234000
8	-5.037653000	-2.138488000	0.029328000

1	-2.853384000	-1.428032000	-0.072500000
1	2.853384000	1.428024000	0.072664000

Table S22. Optimized coordinates of **O17** form at B3PW91/6-31G(d,p) level of theory.

7	-2.716413000	0.272488000	-0.114211000
7	-1.487604000	0.068503000	-0.291993000
6	-3.539715000	-0.819532000	-0.343923000
6	-4.956933000	-0.757490000	-0.134727000
7	-3.238625000	-2.024126000	-0.776955000
7	-5.487759000	-1.916443000	-0.434631000
8	-4.400431000	-2.679326000	-0.833045000
6	-0.707325000	1.211259000	-0.105584000
6	0.707330000	1.211268000	0.105799000
7	-1.116003000	2.457333000	-0.183573000
7	1.115981000	2.457346000	0.183853000
8	-0.000017000	3.205451000	0.000156000
7	1.487625000	0.068515000	0.292155000
7	2.716438000	0.272540000	0.114438000
6	3.539749000	-0.819493000	0.344058000
7	3.238650000	-2.024169000	0.776853000
6	4.956944000	-0.757471000	0.134711000
8	4.400493000	-2.679289000	0.833120000
7	5.487824000	-1.916342000	0.434837000
7	-5.572381000	0.372840000	0.332494000
7	5.572343000	0.372798000	-0.332724000
7	6.949208000	0.584663000	-0.381302000
8	7.261478000	1.718939000	-0.698463000
8	7.663848000	-0.358793000	-0.124593000
7	-6.949254000	0.584669000	0.381006000
8	-7.663858000	-0.358844000	0.124413000
8	-7.261567000	1.718983000	0.697990000
1	-5.031477000	1.218775000	0.465338000
1	5.031409000	1.218696000	-0.465683000

Table S23. Optimized coordinates of **O18** form at B3PW91/6-31G(d,p) level of theory.

7	-4.686546000	0.267250000	0.028068000
7	-3.439396000	0.103063000	0.057793000
6	-5.393557000	-0.682055000	-0.694488000
6	-6.824342000	-0.653741000	-0.785431000
7	-4.955441000	-1.704118000	-1.396231000

7	-7.228684000	-1.652956000	-1.529081000
8	-6.049665000	-2.283652000	-1.896329000
6	-2.766605000	1.109073000	0.754278000
6	-1.412338000	1.022752000	1.204158000
7	-3.219349000	2.310840000	1.031670000
7	-1.087946000	2.159051000	1.775169000
8	-2.194453000	2.936138000	1.660498000
7	-0.615222000	-0.124709000	1.146327000
7	0.615234000	0.124946000	1.146316000
6	1.412348000	-1.022508000	1.204325000
7	1.087942000	-2.158729000	1.775482000
6	2.766618000	-1.108896000	0.754470000
8	2.194457000	-2.935826000	1.660955000
7	3.219368000	-2.310614000	1.032065000
7	-7.572836000	0.294902000	-0.141857000
7	-8.938497000	0.508058000	-0.319222000
8	-9.541135000	-0.296438000	-0.994915000
8	-9.361267000	1.495580000	0.255897000
7	3.439420000	-0.102996000	0.057837000
7	4.686575000	-0.267153000	0.028212000
6	5.393598000	0.682028000	-0.694499000
6	6.824392000	0.653791000	-0.785284000
7	4.955479000	1.703861000	-1.396575000
7	7.228738000	1.652838000	-1.529156000
8	6.049717000	2.283330000	-1.896726000
7	7.572918000	-0.294548000	-0.141274000
7	8.938413000	-0.508323000	-0.319365000
8	9.541023000	0.295807000	-0.995514000
8	9.361087000	-1.495895000	0.255735000
1	-7.110093000	1.045058000	0.357119000
1	7.110108000	-1.044700000	0.357654000